Article

Investigation of Optimum Sustainable Designs for Water Distribution Systems from Multiple Economic, Operational, and Health Perspectives

Mohamed R. Torkomany [1,2] , Hassan Shokry Hassan [1,3] , Amin Shoukry [4,5] , Mohamed Hussein [6,7,*] , Chihiro Yoshimura [8] and Mohamed Elkholy [2]

1 Environmental Engineering Department, Egypt-Japan University of Science and Technology (E-JUST), New Borg El Arab City 21934, Alexandria, Egypt
2 Irrigation Engineering and Hydraulics Department, Alexandria University, Alexandria 11432, Egypt
3 Electronic Materials Researches Department, Advanced Technology and New Materials Research Institute, City of Scientific Research and Technological Applications (SRTA-City), Alexandria 21934, Egypt
4 Computer Science and Engineering Department, Egypt-Japan University of Science and Technology (E-JUST), New Borg El Arab City 21934, Alexandria, Egypt
5 Computer and Systems Engineering Department, Alexandria University, Alexandria 11432, Egypt
6 Department of Building and Real Estate, The Hong Kong Polytechnic University, Hong Kong, China
7 Civil Engineering Department, Faculty of Engineering, Assiut University, Assiut 71516, Egypt
8 Department of Civil and Environmental Engineering, Tokyo Institute of Technology, Tokyo 152-8552, Japan
* Correspondence: mohamed.hussein@connect.polyu.hk

Abstract: Optimizing the design of water distribution systems often faces difficulties due to continuous variations in water demands, pressure requirements, and disinfectant concentrations. The complexity of this optimization even increases when trying to optimize both the hydraulic and the water quality design models. Most of the previous works in the literature did not investigate the linkage between both models, either by combining them into one general model or by selecting any representative solution to proceed from one model to another. This work introduces an integrated two-step framework to optimize both designs while investigating the reasonable network configuration selection from the hydraulic design view before proceeding to the water quality design. The framework is mainly based on a modified version of the multi-objective particle swarm optimization algorithm. The algorithm's first step is optimizing the hydraulic design of the network by minimizing the system's capital cost while maximizing the system's reliability. The second step targets optimizing the water quality design by minimizing both the total consumed chlorine mass and the accumulated differences between actual and maximum chlorine concentrations for all the network junctions. The framework is applied to Safi Network in Yemen. Three scenarios of the water quality design are proposed based on the selected decision variables. The results show a superior performance of the first scenario, based on optimized 24-h multipliers of a chlorine pattern for a flow-paced booster station, compared to the other scenarios in terms of the diversity of final solutions.

Keywords: chlorine dosage; multi-objective optimization; network resilience; particle swarm optimization algorithm; performance metrics; water distribution networks

1. Introduction

Water experts face several challenges when trying to manage the available water resources. One of these challenges is to optimize the design and operation of water distribution systems (WDSs). Designing WDSs is classified as a discrete combinatorial non-deterministic polynomial-time hard (NP-hard) optimization problem. Another difficulty arises when trying to optimize more than one objective while satisfying prespecified constraints [1].

Two types of WDSs design can be identified; the hydraulic design [2–6] and the water quality design [7–9]. As a rule of thumb, several difficulties arise when trying to develop an integrated framework to optimize both designs of WDS. In these types of optimization problems, the formulation of the optimization problem itself, side by side with selecting the appropriate optimization algorithm, poses stress on researchers and engineers to achieve the required numerical accuracy [5,10]. Moreover, the multi-objective criterion used in design frameworks should be carefully selected since it should cover some or all of the economic, reliability, and environmental aspects. For instance, the conflicting nature between network cost, hydraulic reliability, and water quality should be carefully investigated in optimizing WDS design [9]. The obtained solutions are expected to represent the trade-off characteristics among the studied objective functions. The variety of solutions obtained from the design frameworks provides the decision-makers with the flexibility to choose the appropriate design accordingly.

Moreover, the wide variety of formulations available in the literature for designing WDSs, and selecting some or all of the design objectives (e.g., reducing network cost, increasing network reliability, improving water quality, reducing carbon emissions) within the problem formulation lays additional computational burdens. Therefore, it is crucial to develop WDSs design frameworks to achieve the optimum system performance from different sustainable perspectives while using reasonable computational resources. In practice, one of the critical technical limitations is the lack of reliable methods to select the proper network configuration to proceed from the hydraulic design to the water quality design and to choose an adequate representation of the booster station, which injects chlorine in a prespecified place within the network, in the optimization model. Addressing these limitations would benefit researchers and engineers to develop integrated design frameworks for WDSs, specifically when coupling hydraulic and water quality design models into one design framework. Thus, a trial is made in this work to study the linkage between both models using a systematic criterion, as will be discussed later.

Therefore, the main objective of the present work is to develop an integrated framework to obtain a diverse set of reliable and feasible solutions that optimize WDSs hydraulic and water quality designs. The developed framework does not require any parameter tuning or penalty coefficients to investigate the most convenient network configuration from the hydraulic design solutions to proceed to the water quality design step. Another secondary objective is investigating the most convenient set of decision variables for the water quality design step among three different proposed scenarios to reach the most diverse set of solutions. To meet these objectives, the present work introduces a general integrated framework for designing WDSs based on a modified version of MOPSO algorithm [11]. This version of MOPSO algorithm outperforms the original one in terms of convergence and diversity of the final obtained set of non-dominated feasible solutions. The general framework incorporates a two-step WDSs design: the hydraulic and the water quality designs. In the hydraulic design step, the network cost is minimized while maximizing its hydraulic reliability. The total chlorine mass and the accumulated differences between the actual and maximum chlorine concentrations are minimized in the water quality design step. The framework has been applied to a real WDS network in Yemen.

2. Literature Review

In general, the WDSs hydraulic design aims to find the optimum size of pipes, best locations, elevations, sizes and locations of storage tanks, setting of valves, and pumps scheduling while satisfying the pressure head and flow velocity constraints. Many objective functions may be targeted in this design, such as minimizing the total network cost, minimizing the network operational cost, and maximizing the network hydraulic reliability [5,12]. On the other hand, water quality design may comprise finding the optimum placement of contamination sensors, the mass of the disinfectant (e.g., chlorine), locations, and diurnal disinfectant patterns for booster stations while maintaining allowable disinfectants concentration. Many objectives can be targeted here, such as minimizing the

contamination detection time, minimizing the total mass of injected chlorine, minimizing the water age, and minimizing the risk associated with using disinfectants while assuring that the concentration of the disinfectant is within prespecified standard limits [9,13,14].

Several studies in the literature have attempted to combine both hydraulic design and water quality design models of WDSs in a single model. To name a few, In Ref. [15], the authors developed a framework for WDSs design based on minimizing the pumps' operational cost and both turbidity and salinity deviations from standard values. Their framework is mainly based on optimizing the number of working pumps (i.e., ON/OFF scheduling of pumps). In Ref. [16], the authors optimized the design of WDSs in a multi-objective manner, incorporating both the hydraulic design (by optimizing the pump speed) and water quality design (by optimizing the chlorine dosage). They proposed three scenarios to minimize energy and chlorine costs while maximizing the network's hydraulic reliability. In Ref. [17], the authors proposed another integrated multi-objective optimization framework for WDSs design. They optimized the construction cost and a water quality reliability index based on maximizing the disinfectant residuals and minimizing the water age throughout the network. They investigated the optimum pipe diameters, storage tank dimensions, and disinfectant dosage to achieve the earlier objectives. Most of the previous models combined both the hydraulic and water quality models into one single model. However, a variety of different solutions for network configurations may be identified if both models are split into two separate models, paving the way for decision-makers to select the most reasonable and practical configuration for the network among many different options.

Various multi-objective optimization algorithms have been utilized in WDSs optimization problems [1], but none of them have proved superior to others [5,10] since all the optimization algorithms have their pros and cons. For instance, the particle swarm optimization (PSO) algorithm [18], and its multi-objective version (MOPSO) [19] are frequently used to solve WDSs design problems and often lead to satisfactory results. Despite the rapid convergence rate of MOPSO and the small effort needed for its parameters tuning, enhancements are still required to prevent it from falling into local minima and reduce (or even eliminate) the effort required for its parameters tuning [20]. Several attempts were made to enhance MOPSO numerical performance [21,22] or incorporate parts of the PSO algorithm into other state-of-the-art hybrid algorithms such as AMALGAM [23] and GALAXY [6] algorithms.

3. Methodology

3.1. Modified MOPSO Algorithm

Kennedy and Eberhart [18] developed the single-objective PSO algorithm, which imitates the swarm intelligence concept. The algorithm starts with an initial population having a specific number of particles, $jmax$, which move towards the area of optimum solutions. Each particle in the population represents a set of decision variables. Thus, the decision vectors $(x_1, x_2, \ldots, x_j, \ldots, x_{jmax})$ correspond to the positions of all particles. The algorithm iterates to improve the particles' positions by following a leader that moves with the most convenient speed and direction.

The objective function is computed for each particle, and both its personal best value (p_j^{best}) and the global best value over all particles (G^{best}) are stored. Improvement in each particle position is made by changing its personal speed and direction as follows

$$v_{i+1} = w_i v_i + C_1 r_1 \left(p_j^{best} - x_i \right) + C_2 r_2 \left(G^{best} - x_i \right), s.t. v_{max} \leq v_{i+1} \leq v_{min} \tag{1}$$

where, v_{i+1} and v_i are the new and the old particle's velocity vectors, in two consecutive iterations $i + 1$ and i, which should fall between v_{max} and v_{min}, the upper and lower bounds on velocities, respectively, w_i is the inertia coefficient at iteration i, r_1 and r_2 are two random numbers between 0 and 1, C_1 and C_2 are the cognitive and social parameters, respectively

and x_i is the particle's position at iteration i. In most studies, v_{min} is set equal to $-v_{max}$ while w_i is calculated as follows:

$$w_i = 0.5 + \frac{1}{2(\ln(i) + 1)} \tag{2}$$

Then, the position of each particle is updated as follows

$$p_{i+1} = p_i + v_{i+1} \tag{3}$$

where, p_{i+1} and p_i are the new and old particle's positions at iterations $i+1$ and i, respectively.

Afterwards, the algorithm repeats the previous steps for a specific number of iterations, and G^{best} represents the best-obtained solution at the last iteration.

Coello and Lechuga [19] developed the multi-objective PSO algorithm, MOPSO, by extending the single-objective PSO algorithm by adding a repository to store the set of non-dominated solutions at each iteration. At a new iteration, a leader is chosen by the roulette-wheel selection from the stored particles in the repository of the previous iteration. The repository has a specific size, which is equivalent to the population size in this work. The repository particles represent the Pareto front (PF) solutions at a given iteration. Therefore, the final non-dominated solutions are located on the PF obtained at the last iteration.

The optimization constraints are handled as in Ref. [2]. The algorithm selects the repository particles close to or within the search space's feasible region, aiming at moving the whole non-dominated solutions set towards this feasible region. This method performs better at handling the constraints than the penalty method, which needs several trial runs to find the best penalty coefficients, which is computationally expensive and often fails to reach their optimum values.

The algorithm's performance is assessed using the hypervolume metric, HV_m, developed by Ref. [24]. HV_m measures the area of the objective space that the PF covers in every iteration in terms of a reference point. The reference point is selected so that the PF should be of a convex shape. The value of HV_m should increase with the iterations until reaching its maximum value at the last iteration.

When applying the original MOSPSO to the optimization of WDSs, the algorithm usually suffers from premature convergence since it frequently fails to escape from local minima during the search process. Additionally, the original MOPSO algorithm consumes an additional computational budget to perform many trial runs to identify the best values of the PSO parameters, which are C_1, C_2, and v_{max}. Accordingly, a modified MOPSO algorithm was developed in Ref. [11] to enhance its performance in optimizing WDSs design. Several strategies were introduced to the original algorithm, such as self-adaptive PSO parameters [20], a new repository members selection method based on maximizing the overall hypervolume of the final PF generated at the end of each iteration, a regeneration-in-collision strategy to reduce the probability of particles' collision within the objective space and to prevent its premature convergence [25], and an adaptive population size [26,27]. Readers may refer to Ref. [11] for more details. This modified version of MOPSO algorithm is used in the current work.

3.2. Problem Formulation

Designing WDSs is a complex optimization problem since it is a discrete combinatorial NP-hard problem. This complexity is increased when a multi-objective formulation of the problem is needed. In this work, the design of a WDS is divided into hydraulic design and water quality design phases. In all cases, EPANET2.0 [28] is used to simulate the network to get pressure heads and chlorine concentration for each junction and flow velocities and discharges for each pipe. In MOPSO population, each particle position corresponds to a specific network configuration. An EPANET-MATLAB toolkit is utilized to monitor EPANET2.0 from MATLAB [29]. Details about each design step are provided in the following sections.

3.2.1. Hydraulic Design

In this step, each particle decision vector consists of several cells representing the decision variables of this design step, which are all the pipes' diameters in the network along with the storage tanks' location, diameter-to-height ratio, the height of supports, and the pumping power value. A set of the available diameters in the market should be provided, from which all the pipes' diameters should be selected. The size of any storage tank is calculated manually from the required balance between the daily pumped water and the overall daily demand. Pumps of variable speed type account for any daily changes in demand.

The objective functions to be optimized in this step are minimizing the annual network cost (ANC) and maximizing the network resilience (NR). The annual network cost is a function of the annual cost of pipes (APC) along with the annual storage tanks cost (ATC) and the annual pumping energy cost (AEC), as shown in Equation (4).

$$min \text{ ANC} = \text{APC} + \text{ATC} + \text{AEC} \tag{4}$$

$$\text{APC} = \sum_{k=1}^{N_p} C_k(d_{mar}) \times L_k \times CRF, \; mar = 1, \ldots, N_{av} \tag{5}$$

$$\text{ATC} = \sum_{s=1}^{N_{st}} (x_0 + x_1 \, \forall_s + x_2 \, \forall_s \, HS_s) \times CRF \tag{6}$$

$$\text{AEC} = \sum_{p=1}^{N_{ps}} 24 \times 365 \times P_{pu} \, C_e \tag{7}$$

where N_p is the total number of network pipes, C_k is the pipe unit cost per length L_k of pipe k with an available diameter in the market d_{mar}, CRF is the capital recovery factor based on the interest rate and the expected lifetime of the network, N_{av} is the number of available diameters in the market, N_{st} is the number of storage tanks within the network, x_0, x_1, and x_2 are tank cost coefficients, $\forall_s$ is tank s storage volume, HS_s is the height of the supports of tank s, N_{ps} is the total number of pumps, P_{pu} is the pumping power of pump pu, and C_e is the energy unit cost.

The network resilience index (NR) is developed by Todini [30] and updated by Prasad and Park [2]. NR represents the surplus available power for all the network junctions that may confront any upcoming failure due to pipes' bursts, contamination intrusion, etc. NR also includes a uniformity coefficient (U_m) which is calculated for each junction m to check the redundancy of the network pipes. More details on this index can be found in Ref. [2]. The network resilience can be represented by Equation (8).

$$max NR = \frac{\sum_{m=1}^{N_{jun}} U_m Q_m \left(H_m - H_m^{req} \right)}{\left(\sum_{r=1}^{N_{rs}} Q_r H_r + \sum_{pu=1}^{N_{ps}} \frac{P_{pu}}{\gamma} \right) - \sum_{m=1}^{N_{jun}} Q_m H_m^{req}}, \tag{8}$$

where NR is between 0 and 1, N_{jun} is the number of network junctions, Q_m is junction m demand, H_m is junction m piezometric head, H_m^{req} is junction m minimum piezometric head, N_{rs} is the number of network reservoirs and storage tanks, Q_r is the reservoir/storage tank r inflow/outflow, H_r is the water elevation of the reservoir/storage tank r, and γ is the unit weight of water.

The uniformity coefficient (U_m) is calculated as follows:

$$U_m = \frac{\sum_{t=1}^{N_{tp}} d_t}{N_{tp} \times max\{d_t\}} \tag{9}$$

where, N_{tp} is the number of pipes connected to any junction m, and d_t is the diameter of pipe t in which junction m is one of its ends.

The MOPSO algorithm is run to find the feasible non-dominated set of solutions that satisfy maximum and minimum pressure constraints, P_{max} and P_{min}, respectively, for each junction during the simulation time. The MOPSO algorithm is also run to find the pay-off characteristic curve between *ANC* and *NR* by obtaining the final PF from several runs. The final PF particles, obtained from all the runs, are grouped together, and the same non-dominating sorting used in the algorithm is applied to them to get one final accumulated PF. Hereby, the decision-makers should select only one solution from the final accumulated PF for the network's actual implementation. In this work, the median solution of the final accumulated PF is selected, and it is considered one of the best solutions in the hydraulic design step, which is then used in the water quality design step.

3.2.2. Water Quality Design

The injection of disinfectants, such as chlorine, in WDSs is usually performed using the required dosage at a constant rate into the feeding reservoir. However, in many networks where the demand varies with time and location and the reservoir is not at the center of the network, the chlorine decays spatially and temporally, leaving some end users with unsatisfactory levels of chlorine concentrations. Therefore, a booster injection station may be required in a specific place to inject an additional chlorine dosage using a specific injection pattern to overcome the fluctuations in chlorine concentration for all end users. Thus, in this design step, three different water quality scenarios are developed to choose the best among them. The decision vector of the first scenario for each particle consists of 27 values, which represent the 24-h multipliers ranging from 0.0 to 1.0 of a chlorine pattern for a flow-paced booster station, the location of one booster station connected to a random junction, and two base chlorine injection concentrations for both the booster station and the reservoirs. The chlorine pattern of any reservoir is assumed uniform, leaving only the injected chlorine by the booster station to confront any fluctuations of the chlorine requirements within the network. The decision vector for the second scenario is similar to that of the first scenario, except that the multipliers of the chlorine pattern for the booster station are either 0.0 or 1.0. Finally, the decision vector for the third scenario differs from the second scenario only in representing the chlorine pattern for the booster station since the decision vector in this scenario contains only the starting hour and the ending hour for an assumed uniform chlorine pattern of the booster station, while all the other decision variables are kept the same for all design scenarios.

The objective functions here are minimizing both the total daily chlorine mass injected within the network (*DCM*) and the accumulated difference (*ACD*) between the maximum record of the actual chlorine concentration and the maximum allowed chlorine concentration for all network junctions without violating the maximum and minimum permitted chlorine concentrations (CC_{max} and CC_{min}, respectively). *DCM* is evaluated by accumulating all the daily chlorine mass injected at booster stations and reservoirs as follows

$$minDCM = \sum_{kc=1}^{N_c} \sum_{\Delta t=1}^{T} CC_{kc}^{\Delta t} \, Q_{kc}^{\Delta t} \, \Delta t \tag{10}$$

where, N_c is the total number of booster stations and reservoirs in the network, Δt is the prespecified time step in which the results are often recorded, T is a 24 h period in which the chlorine consumption reaches a steady state, and $CC_{kc}^{\Delta t}$ and $Q_{kc}^{\Delta t}$ are the actual chlorine concentration and the outflow of booster station/reservoir kc in time step, Δt, respectively.

The second objective (*min ACD*) aims at minimizing the gap between the maximum chlorine concentration recorded along the 24 h selected period (CC_m^{max}) and the maximum allowed concentration (CC_{max}) for all network junctions to confront any upcoming failures in chlorine concentrations due to any fluctuations in demands and pressures. *ACD* is calculated as follows:

$$minACD = \sum_{m=1}^{N_{jun}} (CC_{max} - CC_m^{max}) \, \beta_m \tag{11}$$

where, β_m is a weighting factor for each junction, m, and may be calculated by dividing the accumulated daily water quantity, $\forall_m^T$, supplied to each junction, m, by the total daily water quantity supplied to all the network, $\forall_{total}$.

As in the hydraulic design step, the MOPSO algorithm is run to find the feasible non-dominated set of solutions that form a PF in each run. The algorithm is run several times, and the final results from all the runs are accumulated to form one final PF for each scenario. Figure 1 summarizes all the steps of the developed framework, including the hydraulic and WQ design.
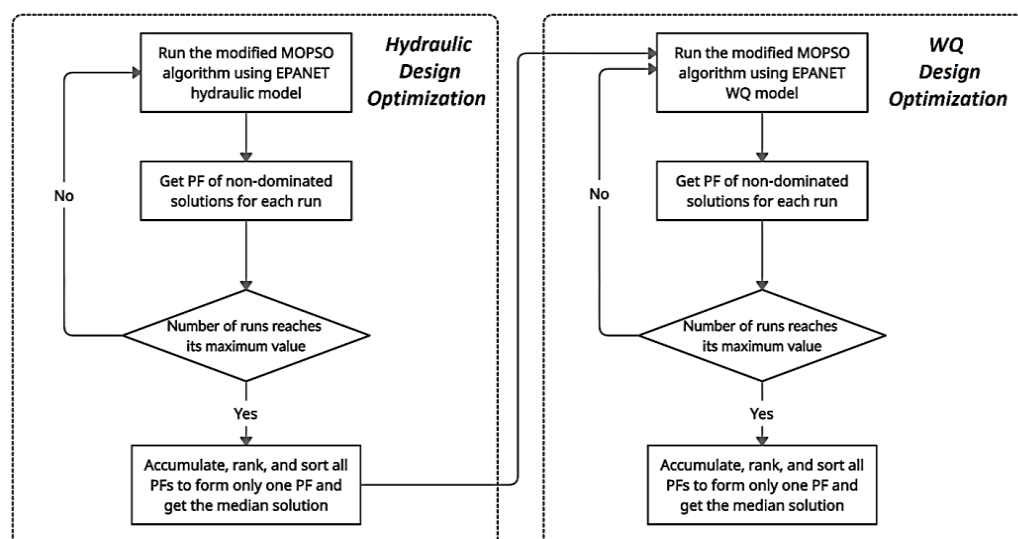

Figure 1. Flow diagram of the general steps describing the developed framework.

4. Case Study and Model Implementation

The developed optimization framework is applied to Safi WDS in Yemen. Figure 2 shows the layout of the town network with pipes and junction IDs in black color, and maximum daily base demands of junctions (l/s) and pipes lengths (m) in red and blue colors, respectively. The network consists of 25 junctions and 35 pipes with 8 available diameters in the market.

The network is fed from a ground tank, which acts as a reservoir. This reservoir is located northeast of the network and is accompanied by a pumping station. The pumping station is assumed to have only one variable speed pump with constant power. All junctions have the same diurnal demand pattern with different base demands except for one junction located far west of the network. This junction in the far west is a factory whose demand starts from 7 am till 7 pm with a uniform demand pattern.

A single storage tank balances the demand to satisfy the diurnal demand pattern fluctuations during any normal operational day. It is worth noting that separate trials were made to investigate the effect of inserting two storage tanks in the network following the same criterion used for a single tank design. However, it was found that most of the results indicated locating one large storage tank side by side with another relatively small storage tank, indicating the insignificance of inserting more than one large tank in the Safi network. More information about the roughness of pipes, allowable pressures of nodes, pipes costs, and design variables limits can be found in Table A1 in the Appendix A, while the demand pattern and elevations of network nodes are shown in Figure A1 in Appendix A.

The minimum and maximum allowed pressure heads, P_{min} and P_{max}, are assumed to be 20 and 60 m, respectively, while the minimum and maximum allowed chlorine concentrations, CC_{min} and CC_{max}, are assumed to be 0.2 and 0.6 mg/L, respectively. The tank cost coefficients, x_0, x_1, and x_2 are set equal to 35×10^4, 150, and 3, respectively.

Each junction's cyclic state for its chlorine concentration pattern for this network is obtained after running the model for one day. The evaluation of the objective functions

for each design step (i.e., the hydraulic design step and the water quality step) is carried out only on the second day of simulation to ensure that a cyclic chlorine pattern is reached for all the junctions. The network resilience (NR) is calculated at 8 pm on the second day, which is the maximum daily demand hour.
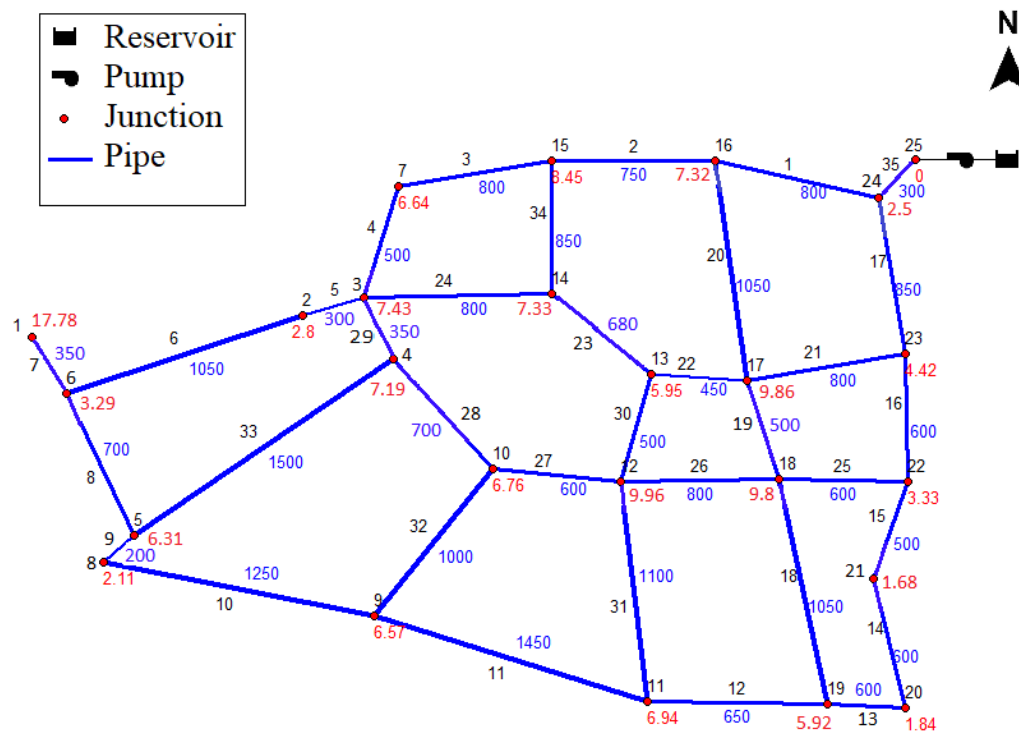

Figure 2. Layout of Safi's water distribution system.

5. Results and Discussion

The modified MOPSO algorithm runs 15 times for each design step, the hydraulic design step and the water quality design step. The final PFs obtained from all the runs are accumulated, ranked, and sorted to form one final PF per design step, as shown in Figure 3. Based on the first scenario of the water quality design step and utilizing the configuration of the median solution for the resultant hydraulic design PF, the final PFs comprise 282 and 200 non-dominated feasible solutions for the hydraulic design and the water quality design, respectively.

Moreover, to investigate the effect of the hydraulic configuration of the network on the water quality design results, other hydraulic configurations from the resulting hydraulic design PF are used to proceed to the water quality design using the first water quality design scenario. These configurations are the first extreme point, the 25% quartile point, the 75% quartile point, and the last extreme point of the final hydraulic design PF, as shown in Figure 3a. In Figure 3b, the resulting water quality PFs from the different hydraulic configurations indicate no direct correlation between the final PF of the hydraulic design and the resulting PFs of the water quality design. This could be attributed to the fact that no clear sequence was identified for the resulting water quality PFs. For instance, the water quality PF based on the 75% quartile point from the hydraulic design dominates all the other resulting PFs in terms of the studied objective functions for the water quality design step. Therefore, the selection of the appropriate network hydraulic configuration should be carefully investigated by designers and decision-makers to reach a competent overall network design.
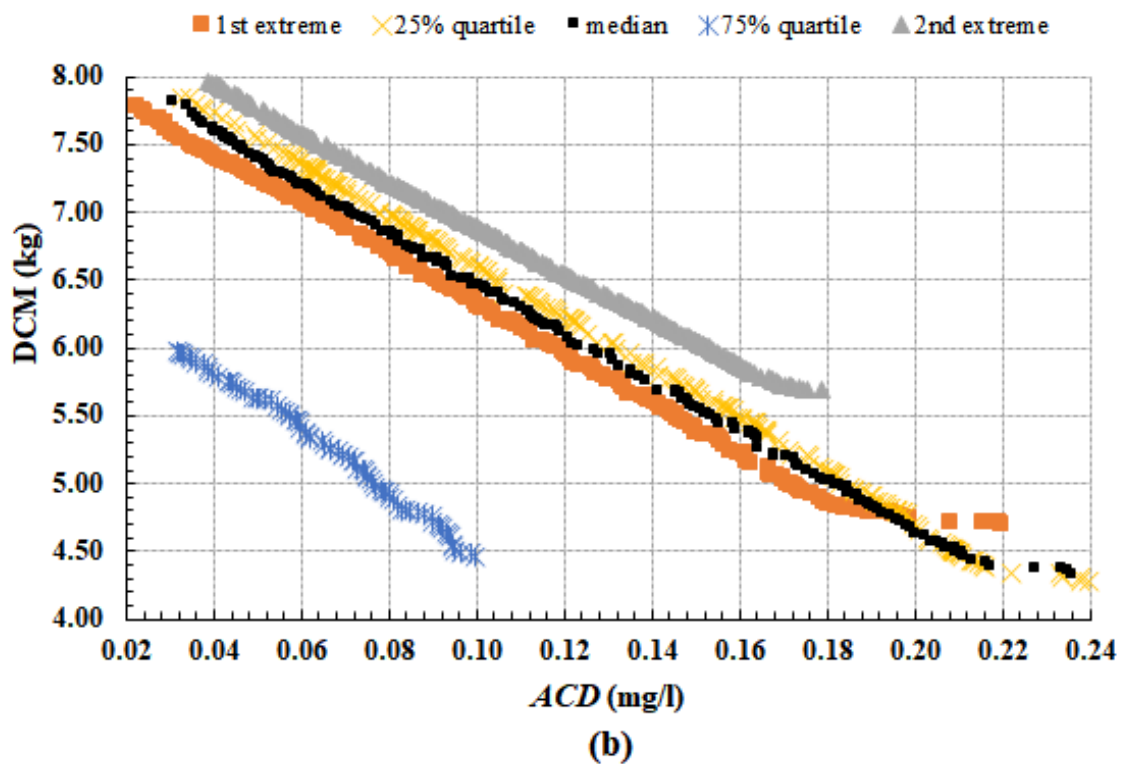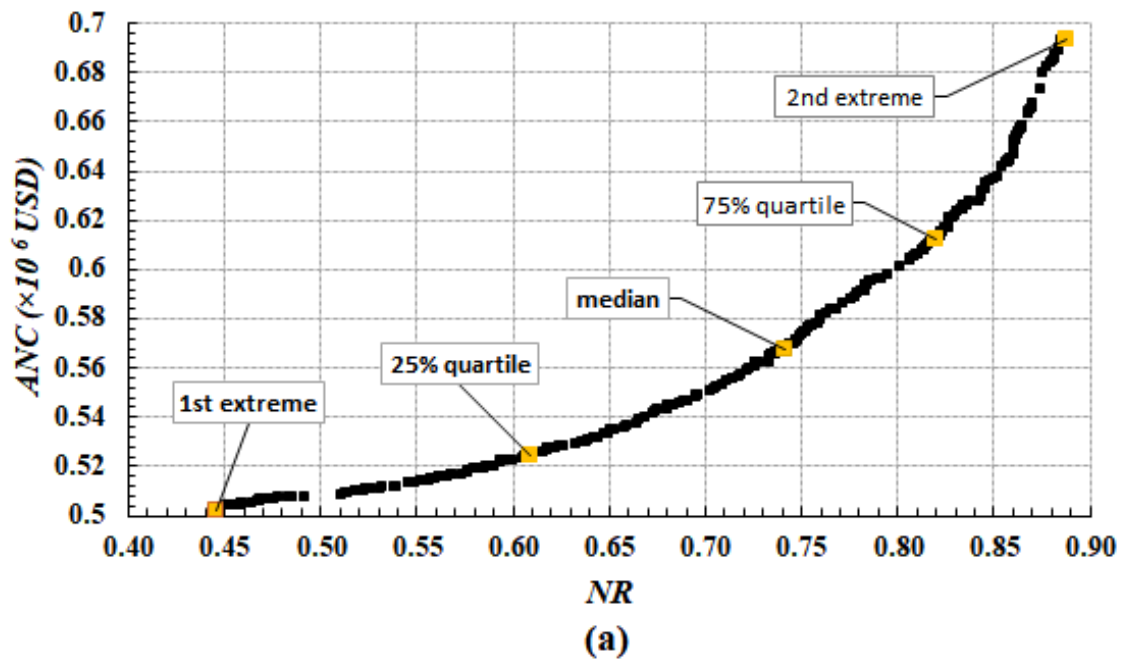
Figure 3. Final PFs of the two design steps (**a**) Hydraulic design, (**b**) First scenario of the water quality design. *NR*: network resilience, *ANC*: annual network cost, *ACD*: accumulated chlorine differences in concentrations for all junctions, *DCM*: daily chlorine mass.

Regarding the different proposed scenarios for the water quality design step, the median solution of the hydraulic design step PF is used to obtain the final water quality PF for each scenario, as shown in Figure 4. The final PF of the first scenario has 200 feasible solutions with HV_m of 1.772. On the contrary, the second and the third scenarios have 279 and 845 feasible solutions with HV_m of 1.36 and 1.65, respectively. The PF of the first scenario ranges from 0.031 mg/L to 0.236 mg/L for *ACD* and from 4.326 kg to 7.823 kg for

DCM, covering the widest range of objective functions values among all the obtained PFs from other scenarios. The second scenario produces the least diverse and convergent PF among all the other scenarios PFs. It only covers a range from 0.142 mg/L to 0.239 mg/L for *ACD* and 4.508 kg to 6.246 kg for *DCM*. The third scenario PF almost has the same range as the first scenario. However, a considerable gap in this PF is noticed, ranging from 0.150 mg/L to 0.201 mg/L for *ACD* and from 5.348 kg to 6.234 kg for *DCM*. All the PFs characteristics for the three scenarios are summarized in Table 1. The first scenario is the most computationally effective. However, it may be classified as the most impractical scenario since it relies on a non-uniform chlorine pattern of the booster station with wide multipliers variability during the one-day operation. Several trials were made to smooth the non-uniform chlorine pattern that resulted from the simulation. However, all the obtained results were found to be infeasible. This indicates that the chlorine concentration is quite sensitive to any change confirming the impracticality of this scenario. The second scenario appears more practical than the first, but its implementation remains challenging due to the difficulty of turning the boosted chlorine on and off. On the other hand, the third scenario is the most practical from the author's perspective, as it is the most commonly implemented by water utilities, despite a significant PF gap. However, the third scenario kept producing infeasible solutions for 6 runs out of the total 15 runs used for obtaining the results in the water quality design step, indicating significant difficulties in converging to the feasible region of the studied search space compared to the first and second scenarios. Therefore, for simplification purposes, the water quality PF resulting from the first scenario based on the median solution configuration from the final hydraulic design PF is utilized to analyze the rest of this work.
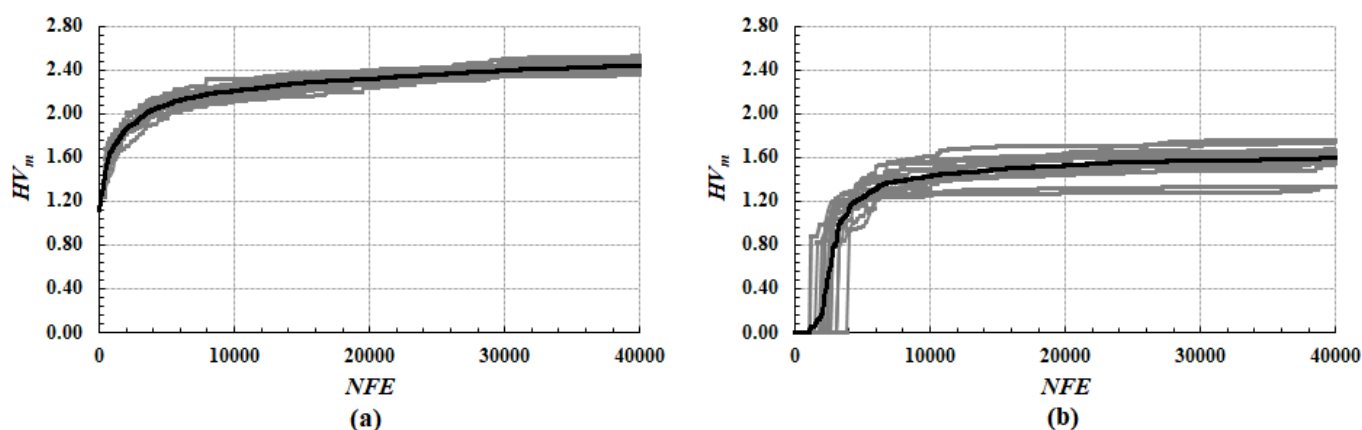
The hypervolume metric, HV_m, progress curves for all the runs for each design step are presented in Figure 5. The HV_m is drawn versus the number of function evaluations, *NFE*. *NFE* represents how many times the algorithm evaluates the objective functions during any single run and also represents the consumed computational budget. An *NFE* of 40,000 is used in any single run for the hydraulic and water quality designs. A mean curve is also drawn in black in the same figure to represent the mean performance of the algorithm.
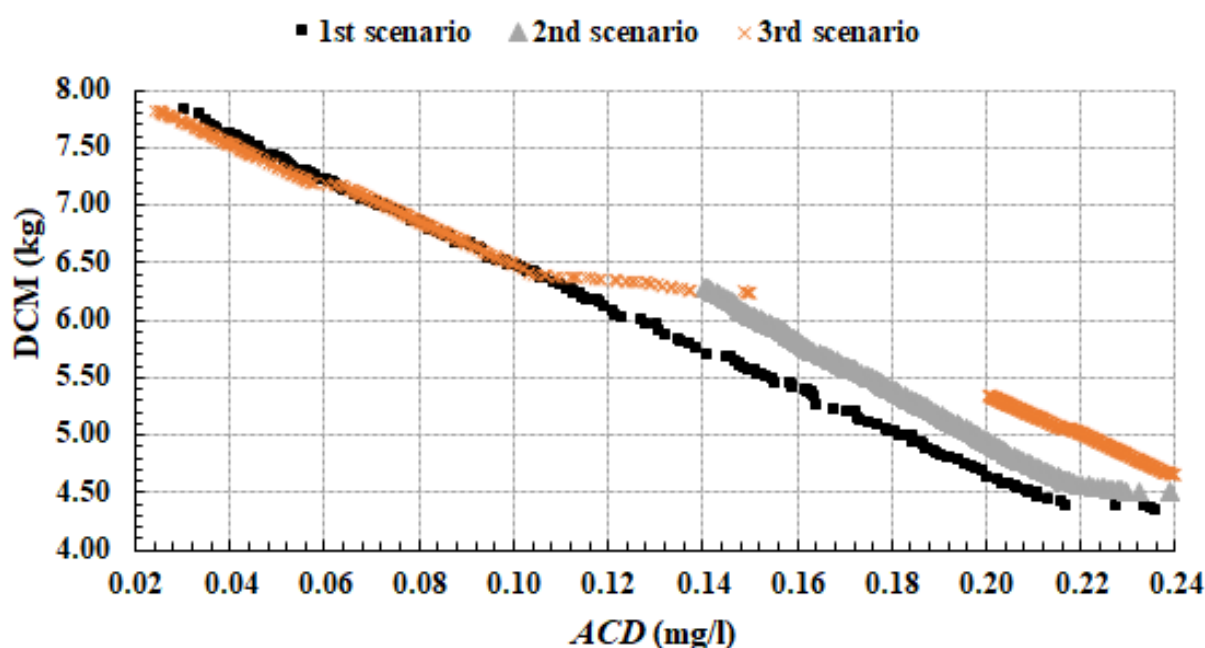
Figure 4. Final PFs of the different proposed scenarios in the water quality design step. *ACD*: accumulated chlorine differences in concentrations for all junctions, *DCM*: daily chlorine mass.

Table 1. A comparison between the final PFs of each design scenario for the water quality design step.

ID	Design Scenario		
	I	II	III
No. of feasible solutions	200	279	845
HV_m	1.772	1.360	1.650
Upper PF point ACD (mg/L)	0.031	0.142	0.024
Lower PF point ACD (mg/L)	0.236	0.239	0.251
Upper PF point DCM (kg)	7.823	6.246	7.829
Lower PF point DCM (kg)	4.326	4.508	4.600

Figure 5. HV_m progress curves for (**a**) Hydraulic design step runs, (**b**) Water quality design step runs. *NFE*: number of function evaluations, *HV*: hypervolume metric.

The algorithm rapidly converges to the area of feasible solutions in the hydraulic design step since it begins to record increasing HV_m values from the beginning of *NFE*. On the contrary, the algorithm consumes relatively more *NFE* at the beginning of any run in the water quality design step to converge to the feasible solutions area compared to the hydraulic design step. The reason for this is that the search space of the water quality design step is larger than that of the hydraulic design step since the former has a wider set of available options for the values of its decision variables.

For the PF of the hydraulic design step, the annual network cost, *ANC*, ranges from 5.02×10^5 to 6.94×10^5 USD, which corresponds to a network resilience, *NR*, varying from 0.45 to 0.89, respectively. Almost 82% of the PF solutions place the storage tank on a small hill in the western part of the network, while the rest of the solutions place it at scattered points west of the network. The PF solutions propose a mean height of tank supports of almost 22.00 ± 3.40 m, a mean ratio of the tank's diameter to height of around 0.92 ± 0.19, and a mean pumping power of 55.48 ± 2.78 kw.

The hydraulic design PF's median solution is representative of all the other solutions. In this solution, the annual network cost, *ANC*, is about 5.67×10^5 USD, and the network resilience, *NR*, is around 0.74. The storage tank in this solution is located above the small hill west of the network. The tank has a support height of about 25.25 m, a diameter of approximately 17.25 m, and the ratio of the tank's diameter to storage height is about 0.80. The pump generates a constant power of roughly 55.50 kw, and the pipes configuration is given in Table 2. The storage tank stores water in low-demand periods while discharging water into the network in high-demand periods.

Table 2. Network pipes configuration of the median solution.

	Pipes				
ID	**35**	**1–2, 17**	**3–5, 15–16, 29**	**6–9, 13–14, 18–23, 25–28, 30, 32, 34**	**10–12, 24, 31, 33**
Diameter (mm)	500	400	300	200	100

For the water quality design step, the extreme points on the PF curve show that *DCM* varies from as low as 4.33 to 7.82 kg, while the corresponding *ACD* value varies from 0.24 mg/L to 0.03 mg/L. The water-quality PF curve exhibits almost a linear trend. All the PF solutions locate the booster station adjacent to the storage tank. The PF solutions introduce mean base concentrations of the booster station and reservoir of around 0.333 mg/L and 0.447 mg/L with standard deviations of ± 0.036 mg/L and ± 0.090 mg/L, respectively.

The median solution of the water quality PF has *DCM* of 6.12 kg per day and *ACD* of about 0.11 mg/L while locating the booster station to the closest junction near the storage tank. The network's water balance and the booster station's chlorine pattern are shown in Figure 6. The negative values in Figure 6 show that the storage tank is in the process of filling, while the positive ones indicate that it is emptying. It may be noticed that there are two peaks in the chlorine pattern for this solution, which oddly match the same timing of the two peaks in the demand pattern. However, after investigating the other PF solutions, it is found that this matching is not supposed to be generalized or considered a rule since there is no direct correlation between the water demands and chlorine concentrations.
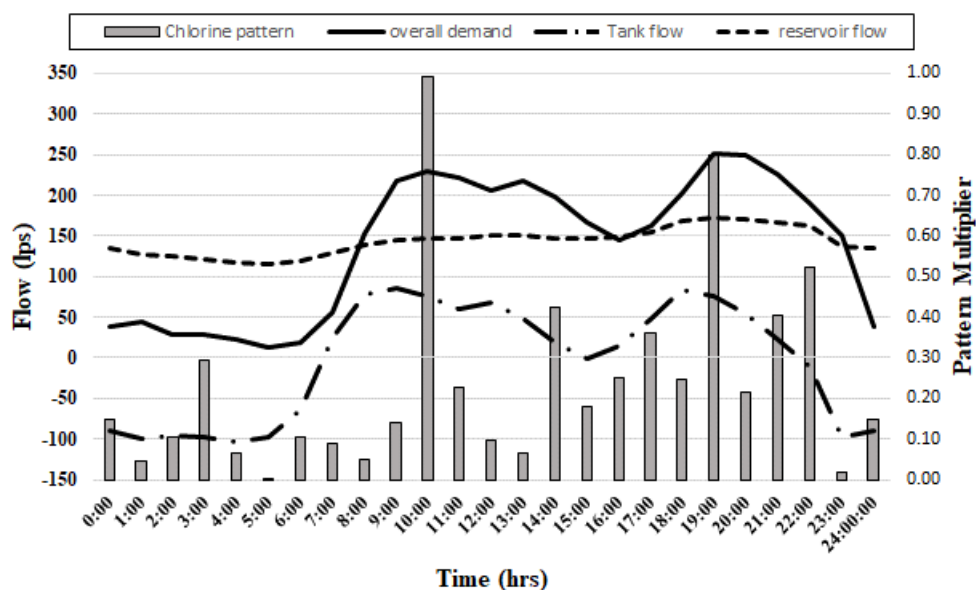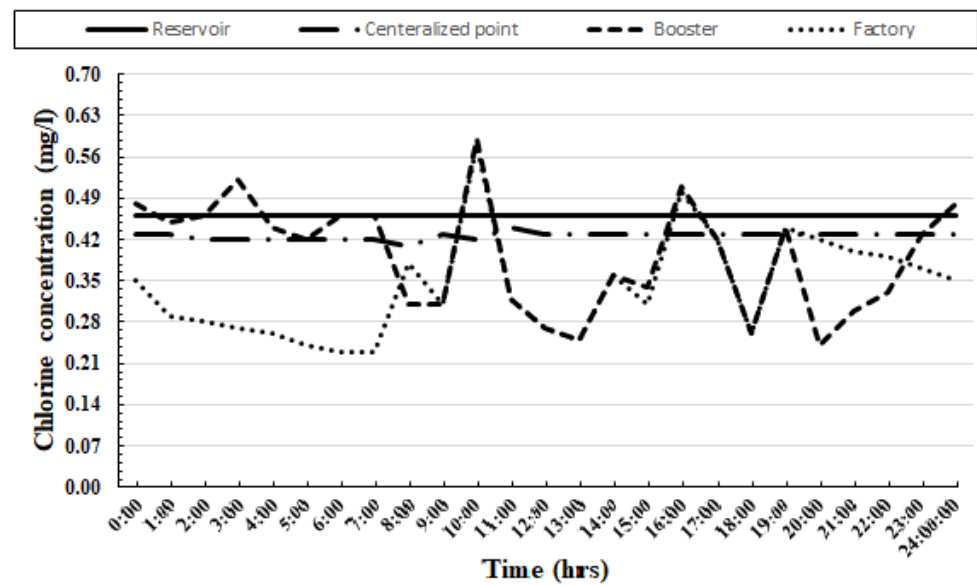

Figure 6. Water balance of the network and chlorine pattern of the booster station for the median solution of the water quality design step.

Figure 7 represents the daily chlorine concentrations for the reservoir, a centralized point, the booster station, and the factory located far west of the network. However, none of the junctions' concentrations violate the chlorine constraints, CC_{min} and CC_{max}, along any hour during the selected simulation day. The configuration of the booster station (i.e., the chlorine pattern, the station location, and the base chlorine concentration) along with the constant chlorine concentration provided by the reservoir satisfy the chlorine requirements along the studied day while pushing the concentration towards the maximum allowed concentration, CC_{max}. This criterion of pushing the actual chlorine concentrations towards CC_{max} alleviates the violations of chlorine constraints that may occur during unusual events (e.g., pipe bursts, pipes leakages, etc.) while maximizing the chlorine residuals at the far ends of the network.

Figure 7. Chlorine concentrations at different points in the network for the median solution of the water quality design step.

Figure 8 shows the mass flow rate of the total chlorine dosage during the studied 24-h time period. The accumulation of both mass flow rate curves for the reservoir and the booster station using a time step of 15 min results in a total chlorine mass of 6.12 kg per day. Relatively larger fluctuations are observed in the mass flow rate curve of the booster station compared to a nearly smooth curve of the reservoir. This is evident since the nodes' concentrations from the east to the center of the network, which have the same demand pattern, are affected by the reservoir concentration. On the contrary, the booster station mainly affects the rest of the network with partially higher fluctuations due to the factory node's variable demands compared to any other ordinary node. Therefore, the reservoir produces a larger chlorine dosage rate with smoother fluctuations, while the booster station produces a smaller one with higher fluctuations.
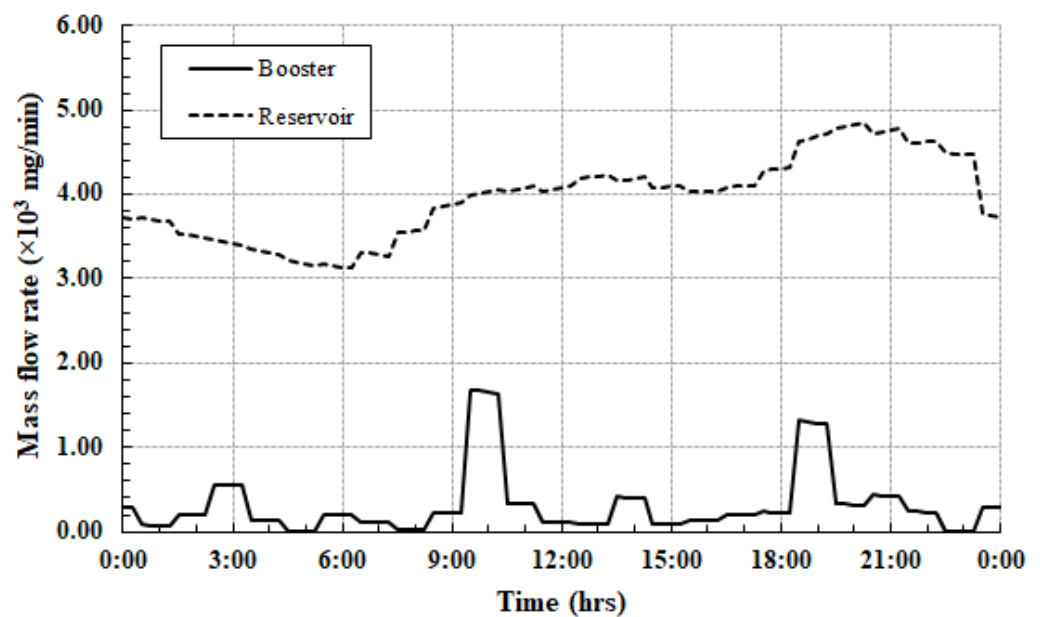
Figure 8. Chlorine mass flow rate for the median solution of the water quality design step.

6. Conclusions

This study aimed to investigate the optimum design of water distribution networks in terms of both hydraulic and water quality design aspects. Most previous works combined both designs into one optimization model, neglecting the effect of splitting the whole optimization process into two separate models, i.e., the hydraulic design and the water quality design models. The splitting process is necessary to investigate the network behavior in each model and obligatory when decision-makers require larger sets of practical and feasible solutions for the studied networks. Accordingly, a two-step design framework based on a modified version of MOPSO algorithm is developed to optimize the network's hydraulic and water quality designs and is applied to a real network in Yemen. In the hydraulic design step, a Pareto set of non-dominated solutions in terms of the network annual cost and the network resilience is obtained. The proposed framework identifies the configurations of pipes diameters, locations, dimensions, and elevation of a single high-elevated tank, and the required pumping power for each solution. Different solutions from the Pareto set of the hydraulic design step are selected as initial configurations for the water quality design step, and the 75% quartile point produced the most convergent Pareto set among all the studied points.

In the water quality design, three different Pareto sets in terms of the overall chlorine mass injected within the network and the accumulated differences between the actual and the maximum chlorine concentrations for all the network junctions using three different design scenarios are obtained. The chlorine pattern, the location, and the base concentration of a single booster station, along with the base chlorine concentration for the feeding reservoir per solution in the Pareto set, are identified. The three scenarios differ only in formulating the chlorine pattern of the booster station. The final PF of the first scenario assumes initial random values between 0.0 and 1.0 for the chlorine pattern multipliers, the second scenario assumes chlorine pattern multipliers of only 0.0 or 1.0, and the third scenario assumes a uniform chlorine pattern with unknown starting and ending times. Each scenario of the three proposed scenarios has its pros and cons. Although the first scenario is impractical due to the large variations in the chlorine pattern of the booster station, it provides the most diverse PF among all the other studied scenarios. The second scenario is more practical than the first one since it provides a sort of ON/OFF injection of chlorine dosage during the daily operation. However, it produces the least diverse PF among all the other obtained PFs from other scenarios. The third scenario, which could be classified as the most practical scenario, has a large gap in its final PF, reducing the number of design options available for decision-makers to cover all the values of the studied objective functions. Therefore, there exist trade-off characteristics between the accuracy and practicality of each water quality design scenario.

Additionally, for the water quality design step, the booster station revealed its capability to confront any expected fluctuations in the chlorine concentrations, especially for any considerably far or relatively large demand points.

In both design steps, the hydraulic design step and the water quality design step, the modified MOPSO algorithm converges rapidly to the area of feasible solutions within the search space, except for some tiny delays in convergence for the water quality design step. These delays are caused by the wider search space of the water quality design problem compared to that of the hydraulic design problem. Generally, the developed framework is a powerful tool for designing water distribution systems and could be applied to any other network. No parameter tuning of the MOPSO algorithm nor penalty coefficient for constraints handling is needed for the developed framework.

The following points are the most important conclusions of this work:

- The PF solutions of the hydraulic design are crucial for obtaining the best PF solutions for the water quality design. They should be clearly investigated before selecting the most appropriate hydraulic design configuration before proceeding to the water quality design step;

- The splitting of the whole WDSs design process into two sequential steps, the hydraulic design and the water quality design, helps provide decision makers with a more diverse set of solutions compared to solving all the variables simultaneously;
- The chlorine booster stations' number, location, and pattern are very important in confronting chlorine decay, especially for relatively far and large demanding points, and the chlorine pattern shape of each booster station has a trade-off characteristic between its accuracy and its practicality.

7. Study Contribution to Theory and Future Work

Despite the availability of various frameworks in the literature for optimizing WDSs design, the developed framework in this work contributes to the theory by investigating the linkage between the hydraulic and water quality designs of WDSs to obtain a diverse set of optimum, reliable, and practical designs to select from. Moreover, it provides a fast-convergent and easy-to-use tool that successfully reaches semi-optimum design solutions while using a relatively small computational budget.

However, the current work has some limitations that may be investigated later, such as comparing the results of the developed framework, which is mainly based on a modified MOPSO algorithm, which may be compared with that of other optimization algorithms, such as NSGA-II, GALAXY, etc. Moreover, the investigation of water chlorine concentration in the storage tank was neglected, the insertion of more than one storage tank or more than one chlorine booster station was not included, and the seasonal variations in water demands were not considered.

Regarding future works, more objective functions, such as minimizing water leakages, minimizing water age, etc., may be added to the framework to enhance the utility of the proposed framework. Additionally, the same design procedures and guidelines used in this work may be applied to other benchmarks and real WDSs to ensure the applicability of the developed framework.

Author Contributions: Conceptualization, M.R.T., H.S.H., A.S., C.Y. and M.E.; Methodology, M.R.T.; Software, M.R.T.; Formal analysis, M.R.T.; Writing—original draft, M.R.T.; Writing—review & editing, H.S.H., A.S., M.H., C.Y. and M.E.; Visualization, M.R.T.; Supervision, H.S.H., A.S., C.Y. and M.E. All authors have read and agreed to the published version of the manuscript.

Institutional Review Board Statement: Not applicable.

Data Availability Statement: Some or all of the data, models, or code that support this study's findings are available from the corresponding author upon reasonable request.

Conflicts of Interest: The authors declare no conflict of interest.

Appendix A

**Table A1.** Values of the Safi network coefficients and constraints.

Parameter	Description	Value	Unit
Pr_{min}	min. allowable pressure head	20	m
Pr_{max}	max. allowable pressure head	60	m
Vel_{min}	min. allowable flow velocity	0.30	m/s
Vel_{max}	max. allowable flow velocity	1.50	m/s
HS_{max}	max. tank bottom elevation	50	m

Table A1. *Cont.*

Parameter	Description	Value	Unit
P_{max}	max. pump power	200	kw
C_k	Pipe unit cost (d = 80 mm)	60	USD/m
	Pipe unit cost (d = 100 mm)	70	USD/m
	Pipe unit cost (d = 150 mm)	90	USD/m
	Pipe unit cost (d = 200 mm)	130	USD/m
	Pipe unit cost (d = 300 mm)	180	USD/m
	Pipe unit cost (d = 400 mm)	260	USD/m
	Pipe unit cost (d = 500 mm)	310	USD/m
	Pipe unit cost (d = 600 mm)	360	USD/m
N_{av}	Number of available diameters	8	-
C_e	energy unit cost	0.15	USD/kwh
I	interest rate	8	%
N	lifetime	20	years
C_{HW}	Hazen–Williams coefficient	140	-
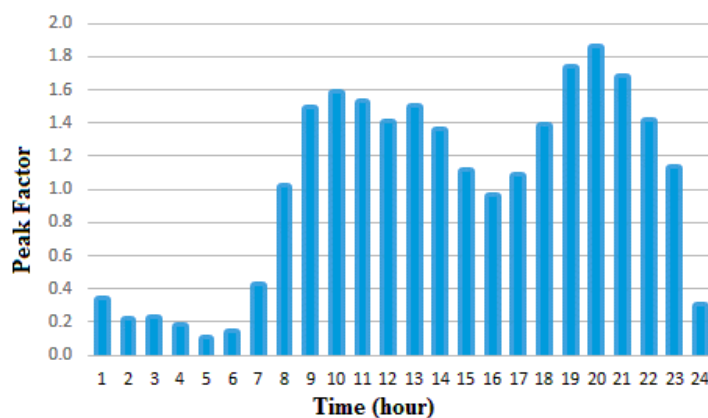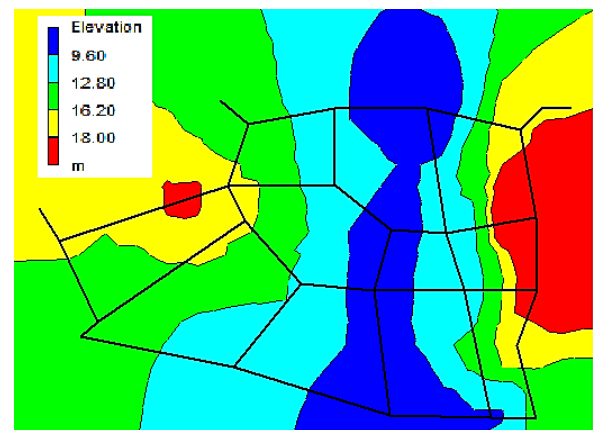
(**a**)　　　　　　　　　　　　　　　　　　(**b**)

Figure A1. (**a**), Safi network demand pattern for all the ordinary nodes, except for node no. 1, which is a factory with a constant demand peak factor of 1.0 from 7 am till 7 pm only, (**b**) contour plot of the Safi network elevations.

References

1. Mala-Jetmarova, H.; Sultanova, N.; Savic, D. Lost in optimisation of water distribution systems? A literature review of system operation. *Environ. Model. Softw.* **2017**, *93*, 209–254. [CrossRef]
2. Prasad, T.D.; Park, N.-S. Multiobjective Genetic Algorithms for Design of Water Distribution Networks. *J. Water Resour. Plan. Manag.* **2004**, *130*, 73–82. [CrossRef]
3. Farmani, R.; Godfrey, W.A.; Savic, A.D. Trade-off between Total Cost and Reliability for Anytown Water Distribution Network. *J. Water Resour. Plan. Manag.* **2005**, *131*, 161–171. [CrossRef]
4. Marchi, A.; Salomons, E.; Ostfeld, A.; Kapelan, Z.; Simpson, A.R.; Zecchin, A.C.; Maier, H.R.; Wu, Z.Y.; Elsayed, S.M.; Song, Y.; et al. Battle of the Water Networks II. *J. Water Resour. Plan. Manag.* **2014**, *140*, 4014009. [CrossRef]
5. Wang, Q.; Guidolin, M.; Savic, D.; Kapelan, Z. Two-Objective Design of Benchmark Problems of a Water Distribution System via MOEAs: Towards the Best-Known Approximation of the True Pareto Front. *J. Water Resour. Plan. Manag.* **2015**, *141*, 4014060. [CrossRef]
6. Wang, Q.; Savić, D.A.; Kapelan, Z. GALAXY: A new hybrid MOEA for the optimal design of Water Distribution Systems. *Water Resour. Res.* **2017**, *53*, 1997–2015. [CrossRef]
7. Boccelli, D.L.; Tryby, M.E.; Uber, J.G.; Rossman, L.A.; Zierolf, M.L.; Polycarpou, M.M. Optimal scheduling of booster disinfection in water distribution systems. *J. Water Resour. Plan. Manag.* **1998**, *124*, 99–111. [CrossRef]
8. Prasad, T.D.; Walters, G.A.; Savic, D.A. Booster disinfection of water supply networks: Multiobjective approach. *J. Water Resour. Plan. Manag.* **2004**, *130*, 367–376. [CrossRef]

9. Farmani, R.; Walters, G.; Savic, D. Evolutionary multi-objective optimization of the design and operation of water distribution network: Total cost vs. reliability vs. water quality. *J. Hydroinformatics* **2006**, *8*, 165–179. [CrossRef]

10. Monsef, H.; Naghashzadegan, M.; Jamali, A.; Farmani, R. Comparison of evolutionary multi objective optimization algorithms in optimum design of water distribution network. *Ain Shams Eng. J.* **2019**, *10*, 103–111. [CrossRef]

11. Torkomany, M.R.; Hassan, H.S.; Shoukry, A.; Abdelrazek, A.M.; Elkholy, M. An Enhanced Multi-Objective Particle Swarm Optimization in Water Distribution Systems Design. *Water* **2021**, *13*, 1334. [CrossRef]

12. Mehzad, N.; Tabesh, M.; AtaeeKia, B.; Hashemi, S. Optimum Reliable Operation of Water Distribution Network Considering Pumping Station and Tank. *Iran. J. Sci. Technol. Trans. Civ. Eng.* **2019**, *43*, 413–427. [CrossRef]

13. Al-Zahrani, M.A. Optimizing dosage and location of chlorine injection in water supply networks. *Arab. J. Sci. Eng.* **2016**, *41*, 4207–4215. [CrossRef]

14. He, G.; Zhang, T.; Zheng, F.; Zhang, Q. An efficient multi-objective optimization method for water quality sensor placement within water distribution systems considering contamination probability variations. *Water Res.* **2018**, *143*, 165–175. [CrossRef] [PubMed]

15. Mala-Jetmarova, H.; Barton, A.; Bagirov, A. Impact of water-quality conditions in source reservoirs on the optimal operation of a regional multiquality water-distribution system. *J. Water Resour. Plan. Manag.* **2015**, *141*, 4015013. [CrossRef]

16. Babaei, N.; Tabesh, M.; Nazif, S. Optimum reliable operation of water distribution networks by minimising energy cost and chlorine dosage. *Water SA* **2015**, *41*, 149–156. [CrossRef]

17. Shokoohi, M.; Tabesh, M.; Nazif, S.; Dini, M. Water quality based multi-objective optimal design of water distribution systems. *Water Resour. Manag.* **2017**, *31*, 93–108. [CrossRef]

18. Kennedy, J.; Eberhart, R. Particle swarm optimization. In Proceedings of the ICNN'95—International Conference on Neural Networks, Perth, Australia, 27 November–1 December 1995; Volume 4, pp. 1942–1948. [CrossRef]

19. Coello Coello, C.A.; Lechuga, M.S. MOPSO: A proposal for multiple objective particle swarm optimization. In Proceedings of the 2002 Congress on Evolutionary Computation. CEC'02 (Cat. No.02TH8600), Honolulu, HI, USA, 12–17 May 2002; Volume 2, pp. 1051–1056. [CrossRef]

20. Montalvo, I.; Izquierdo, J.; Pérez-García, R.; Herrera, M. Improved performance of PSO with self-adaptive parameters for computing the optimal design of Water Supply Systems. *Eng. Appl. Artif. Intell.* **2010**, *23*, 727–735. [CrossRef]

21. Padhye, N. Comparison of Archiving Methods in Multi-Objectiveparticle Swarm Optimization (MOPSO): Empirical Study. In Proceedings of the 11th Annual Conference on Genetic and Evolutionary Computation; Association for Computing Machinery: New York, NY, USA, 2009; pp. 1755–1756. [CrossRef]

22. Deb, K.; Padhye, N. Enhancing performance of particle swarm optimization through an algorithmic link with genetic algorithms. *Comput. Optim. Appl.* **2014**, *57*, 761–794. [CrossRef]

23. Vrugt, J.A.; Robinson, B.A. Improved evolutionary optimization from genetically adaptive multimethod search. *Proc. Natl. Acad. Sci. USA* **2007**, *104*, 708–711. [CrossRef]

24. Zitzler, E.; Thiele, L. Multiobjective optimization using evolutionary algorithms—A comparative case study. In *Proceedings of the Parallel Problem Solving from Nature—PPSN V.*; Eiben, A.E., Bäck, T., Schoenauer, M., Schwefel, H.-P., Eds.; Springer: Berlin/Heidelberg, Germany, 1998; pp. 292–301.

25. Surco, D.F.; Vecchi, T.P.B.; Ravagnani, M.A.S.S. Optimization of water distribution networks using a modified particle swarm optimization algorithm. *Water Supply* **2017**, *18*, 660–678. [CrossRef]

26. DeBao, C.; ChunXia, Z. Particle swarm optimization with adaptive population size and its application. *Appl. Soft Comput.* **2009**, *9*, 39–48. [CrossRef]

27. Hadka, D.; Reed, P. Borg: An Auto-Adaptive Many-Objective Evolutionary Computing Framework. *Evol. Comput.* **2012**, *21*, 231–259. [CrossRef] [PubMed]

28. Rossman, L.A. *EPANET 2: Users' Manual*; US Environmental Protection Agency, Office of Research and Development: Cincinnati, OH, USA, 2000.

29. Eliades, D.G.; Kyriakou, M.; Vrachimis, S.G.; Polycarpou, M.M. EPANET-MATLAB Toolkit: An Open-Source Software for Interfacing EPANET with MATLAB. In Proceedings of the Computing and Control for the Water Industry CCWI 2016, Amsterdam, The Netherlands, 7–9 November 2016.

30. Todini, E. Looped water distribution networks design using a resilience index based heuristic approach. *Urban Water* **2000**, *2*, 115–122. [CrossRef]